An Unsteady Model to Study the Effects of Porosity and Temperature in All-Vanadium Redox Flow Battery with Mass Transfer and Ion Diffusion

H. M. Sathisha and Amaresh Dalal

Abstract The crossover of vanadium ions through membrane in vanadium redox flow battery after many cycles leads to capacity loss of the cell. Different membrane materials show different diffusion behavior which results in variation in the cell potential response. The diffusion coefficients of the membrane is temperature dependent, therefore, concentration profile varies with temperature. The model has considered the effects of crossover of vanadium ions through membrane and mass transfer. The present model predicts the capacity loss for different membrane materials. The simulation results show that reaction rate constants and diffusion coefficients depend on temperature and these affect the cell performance. The results show that for Selemion AMV and Selemion CMV membranes capacity loss increases linearly at different temperatures and porosity with increase in number of cycles. In the case of Nafion 115 membrane the capacity decays up to 77 cycles and then it stabilizes.

Keywords Mass transfer · Crossover · Porosity · Temperature
Cell potential

1 Introduction

Redox flow batteries are more popular because they offer various advantages. The advantages are high energy efficiency, elimination of electrolyte cross-contamination, long cycle life, active thermal management, low cost for large energy storage systems, etc. [1, 2]. One more important feature of redox flow batteries is that the flexibility of power and capacity design of a battery are not

H. M. Sathisha · A. Dalal (✉)
Department of Mechanical Engineering, Indian Institute of Technology Guwahati, Guwahati 781039, Assam, India
e-mail: amaresh@iitg.ernet.in

H. M. Sathisha
e-mail: m.sathisha@iitg.ernet.in

S. De et al. (eds.), *Sustainable Energy Technology and Policies*,
Green Energy and Technology, https://doi.org/10.1007/978-981-10-8393-8_17

coupled which makes it efficient design of the battery configurations. Therefore, the redox flow batteries are suitable for the applications of peak shaving, load leveling, grid integration and frequency regulation [1–5]. Compared to other flow batteries, all-vanadium redox flow battery (VRFB) is more popular because there is no problem of electrolyte cross-contamination due to the fact that both the half cells of the battery employ different species of vanadium in the electrolyte. As a result electrolyte lifetime is considerably increased. Also it is found that from VRFB the disposal of vanadium ions will not create any environmental issues in comparison with conventional lead acid battery.

A VRFB has vanadium ions reacting in two half cells of the battery, each cell being separated by an ion exchange membrane which only allows proton ions to pass through to make charge balance. An ideal proton exchange membrane should possess chemical stability, good conductivity, and also control the flow of vanadium ions from negative half cell to positive half cell or vice versa.

After using VRFB for many cycles the performance reduces due to ion diffusion of vanadium ions pass through membrane. Therefore, a lot of research is going on to improve performance and maintain the capacity for long term cycling. It was found that no membrane gives 100% performance [6], there will be vanadium ions diffusion through membrane from negative half cell to positive half cell and vice versa. Due to diffusion of vanadium ions, the vanadium concentration of one half cell increases and the other half cell vanadium concentration decreases, which results in performance loss of the cell. Due to self discharge reactions, capacity of the cell decreases and this can be restored by remixing the vanadium ions to both half cells periodically. Also there is oxygen and hydrogen evolution side reactions taking place inside the cell, which results in capacity loss, to restore the capacity it requires electrochemical rebalance. Several researchers proposed few approaches to overcome the performance loss for different operating conditions of the cell. Studies have shown that crossover of vanadium and water through membrane reduce the coulombic efficiency and capacity. Numerical model has been developed to study the effect of self-discharge for VRFB [7]. Two-dimensional isothermal numerical model including the effect of crossover and water through membrane shows the capacity loss of the battery [8]. Tang et al. [9] developed a model in which the approach is based on molar mass balance simplified equations for studying self discharge process and they studied the effect of diffusion coefficients, flow rate and concentration of hydrogen ions. Same model is extended by adding the energy balance equation, model predicts capacity loss and temperature of electrolyte for a Nafion 115 membrane [10]. The model employed Arrhenius equation to model the temperature dependent diffusion coefficients of membrane. Badrinarayanan et al. [6] studied the model for ion diffusion and the effects of temperature and electrolyte transfer. One more model is developed for the self discharge process of the vanadium redox flow battery [11], the model includes mass transfer and vanadium ions crossover through the membrane, they showed the effects of temperature on crossover.

The present simulation is based on model developed by Yu and Chen [11], including the effects of mass transfer and crossover of vanadium ions through

membrane. The effects of temperature on diffusion coefficients and effects of porosity on concentration for different membrane materials using this model have not been studied so far. Three membranes are used in the simulation which includes Selemion CMV, Selemion AMV and Nafion 115 membrane. These membranes are available in the market and most of the researchers are used in their experiments and numerical simulation [9]. The main difference between these membrane materials is the difference in diffusion coefficients. Due to the variation in diffusion the crossover of vanadium ions also varies for different membrane materials.

2 Principles of Operation and Model Assumptions

VRFB includes three major components as shown in Fig. 1a: (i) two porous electrodes that act as active sites for redox reactions, (ii) liquid electrolytes that include of different vanadium ions dissolved in sulphuric acid solution, and (iii) a proton exchange membrane that serves as a separator to prevent the cross-over of the vanadium ions from both the positive and the negative half-cells.

The following main electrochemical reactions taking place at each electrode
At the negative electrode

$$V^{3+} + e^{-} \rightleftharpoons V_2^{+} \tag{1}$$

At the positive electrode

$$VO^{2+} + H_2O - e^{-} \rightleftharpoons VO_2^{+} + 2H^{+} \tag{2}$$

The following are the self-discharge reactions occurred at each of the electrode
At negative electrode

$$V^{2+} + VO^{2+} + 2H^{+} \rightarrow 2V^{3+} + H_2O \tag{3}$$

$$2V^{2+} + VO_2^{+} + 4H^{+} \rightarrow 3V^{3+} + 2H_2O \tag{4}$$

$$V^{3+} + VO_2^{+} \rightarrow 2VO^{2+} \tag{5}$$

At positive electrode

$$2VO_2^{+} + V^{2+} + 2H^{+} \rightarrow 3VO^{2+} + H_2O \tag{6}$$

$$VO_2^{+} + V^{3+} \rightarrow 2VO^{2+} \tag{7}$$

$$VO^{2+} + V^{2+} + 2H^{+} \rightarrow 2V^{3+} + H_2O \tag{8}$$

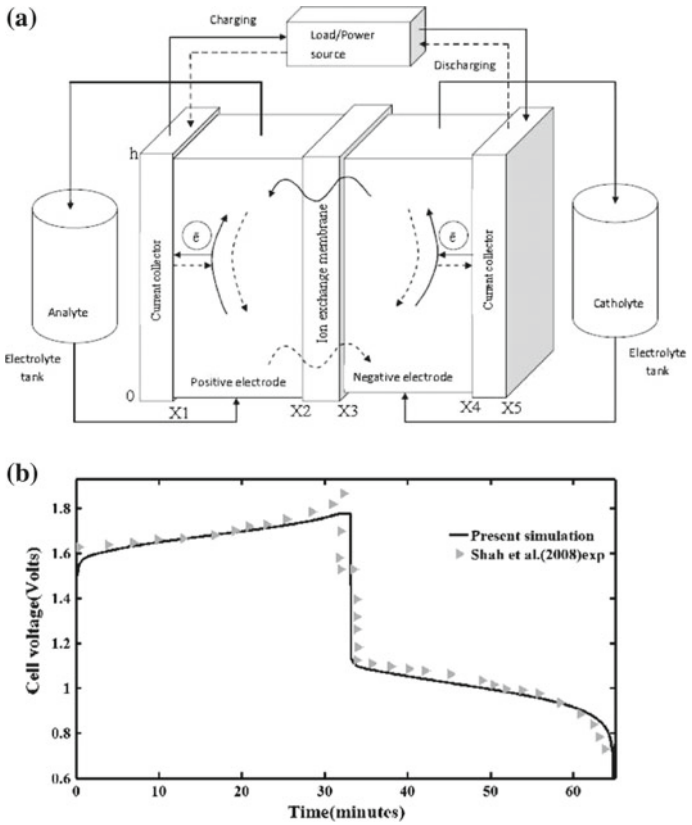

Fig. 1 **a** Schematic of the all-vanadium redox flow battery showing the components, current collectors, porous electrodes, membrane and reservoirs. **b** Comparison between simulated and experimental cell voltage variation. The vanadium concentration was 1200 mol/m^3, the current density was 1000 A/m^2, the cell temperature was 297 K and the flow rate was 1×10^{-6} m^3/s

After many cycles, concentration imbalance takes place in the battery due to difference in diffusion rates of vanadium ions. Vanadium crossover occurs between two half cells through membrane which results in loss of performance of cell [9]. Water crossover affects on the overall concentration of vanadium in both half of cell. Here water crossover is neglected and this can be overcome by approximating the effective diffusion coefficient of vanadium species.

The following are the assumptions considered for simplifying the equation.

1. Apart from oxidation-reduction reactions there will be hydrogen and oxygen gas evolving reactions occur under normal conditions [12, 13].
2. Vanadium ions are diffused through the membrane and react instantaneously; therefore side reactions are considered.
3. Water crossover is neglected due to difficulty in predicting the electro-osmatic drag and osmosis by lumped model.

3 Model Equations

The equations are based on law of conservation of mole for vanadium species in the electrodes and reservoir volumes of each half cell. Due to diffusion in the membrane, the concentration of vanadium changes in the porous electrode by recirculation of electrolytes between the reservoir and electrode and externally applied current. The model contains total eight unknowns of concentrations, four for positive and negative porous electrodes and four for concentrations in the external reservoirs. Therefore, the mass balance of species i in the reservoir can be written as,

$$\frac{dC_i^{res}}{dt} = \frac{Q}{V_{res}}(C_i - C_i^{res}) \tag{9}$$

where C_i^{res} and C_i are the respective concentrations in the reservoir and cell of species $i \in [2–5]$ corresponding to V^{2+}, V^{3+}, VO_2^+ and VO^{2+}, respectively, V_{res} is the volume of electrolyte in the reservoir, Q is the electrolyte flow rate.

The mass balance for species includes electrochemical reaction, recirculation and diffusion of species through membrane and these are expressed as,

$$\frac{dC_2}{dt} = \frac{Q}{\varepsilon V_e}(C_2^{res} - C_2) + \frac{A_m j}{\varepsilon V_e F} - \frac{A_m}{w_m}(D_2 c_2 + 2D_5 c_5 + D_4 c_4) \tag{10}$$

$$\frac{dC_3}{dt} = \frac{Q}{\varepsilon V_e}(C_3^{res} - C_3) - \frac{A_m j}{\varepsilon V_e F} - \frac{A_m}{w_m}(D_3 c_3 - 3D_5 c_5 - 2D_4 c_4) \tag{11}$$

$$\frac{dC_4}{dt} = \frac{Q}{\varepsilon V_e}(C_4^{res} - C_4) - \frac{A_m j}{\varepsilon V_e F} - \frac{A_m}{w_m}(D_4 c_4 - 3D_2 c_2 - 2D_3 c_3) \tag{12}$$

$$\frac{dC_5}{dt} = \frac{Q}{\varepsilon V_e}(C_5^{res} - C_5) + \frac{A_m j}{\varepsilon V_e F} - \frac{A_m}{w_m}(D_5 c_5 + 2D_2 c_2 + D_3 c_3) \tag{13}$$

where V_e is volume of the electrode, A_m is the contact area of the membrane, j is the applied current density, ε is the porosity of the electrode, w_m width of the membrane, and D_2, D_3, D_4 and D_5 are the diffusion coefficients of membrane corresponding to respective vanadium species.

The diffusion coefficients depend on temperature and these are approximated using Arrhenius law given by,

$$D = D_0 e^{\frac{E_a}{R}\left(\frac{1}{298} - \frac{1}{T}\right)} \tag{14}$$

where D_0 is the diffusion for each vanadium species at temperature 298K, E_a is the activation energy. Also K_2, K_3, K_4, K_5 are the diffusion coefficients of membrane material at reference temperature 298K, corresponding to respective vanadium species, the values of diffusion coefficients are given in Table 1. It is understood

Table 1 Values of diffusion coefficients for three different membrane materials [9]

Membrane	k_2 (dm/s)	k_3 (dm/s)	k_4 (dm/s)	k_5 (dm/s)
Selemion AMV	3.53×10^{-8}	2.18×10^{-8}	0.91×10^{-8}	2.57×10^{-8}
Selemion CMV	3.17×10^{-7}	0.716×10^{-7}	2×10^{-7}	1.25×10^{-7}
Nafion 115	6.9×10^{-7}	2.54×10^{-7}	5.37×10^{-7}	4.64×10^{-7}

from Eq. 14, the diffusion coefficients of membrane varies exponentially with temperature, this phenomena explained elaborately in results and discussion section. The value of E_a is 1.663×10^4 J/mol taken from literature [14] based on experimental data.

The open circuit voltage is calculated from the Nernst equation given by,

$$E_{OC} = (E^0_{pos} - E^0_{neg}) + \frac{RT}{F} ln\left(\frac{c_2 c_5 c^2_{H+}}{c_3 c_4}\right) \tag{15}$$

where E^0_{neg} and E^0_{pos} are the standard cell potentials for the reactions for negative and positive electrodes, F is the Faraday constant, T is the cell temperature, R is the gas constant and c_{H+} is the concentration of protons in the positive half cell. Due to complex ionic equilibria it is very difficult to model accurately the dynamics of proton concentration. However, the small changes in proton concentration will not affect on cell voltage significantly, therefore proton concentration is assumed to be constant, the value is taken to be 4M for simulations.

The cell voltage E_{cell} is determined by deducting the voltage losses due to ohmic resistance, and activation overpotential to the open circuit voltage, which is given by

$$E_{Cell} = E_{OC} - \sum E_{ohm} - \sum E_{act} \tag{16}$$

Ohmic losses associated with current collector, membrane and electrolyte can be calculated by,

$$E_c = j_{app} \frac{w_c}{\sigma_c} \tag{17}$$

$$E_m = j_{app} \frac{w_m}{\sigma_m} \tag{18}$$

$$E_e = j_{app} \frac{w_e}{\varepsilon^{3/2} \sigma_e} \tag{19}$$

where, σ_c,σ_m, and σ_e are the conductivities and w_c, w_e and w_m are the widths of the current collector, electrode, and membrane respectively. The effective conductivity of electrolyte $\varepsilon^{3/2}\sigma_e$, is obtained by using a Bruggeman correction. For Nafion 115

membrane conductivity can be calculated using the following empirical relationship given by [15],

$$\sigma_m = (0.5139\lambda - 0.326)\exp\left(1268\left[\frac{1}{303} - \frac{1}{T}\right]\right) \tag{20}$$

The membrane conductivity depends on membrane water content λ and temperature of cell. The membrane is assumed to be fully saturated (λ) since, there is constant contact with liquid electrolytes on each side of the cell.

To drive the electrochemical reaction requires overpotential which is calculated from the current-overpotential equation at a given current density assuming equal charge coefficients ($\alpha = 0.5$) [16]

$$\frac{j}{j_0} = \left(1 - \frac{j}{j_{1,c}}\right)\exp\left(-\frac{F\eta}{2RT}\right) - \left(1 - \frac{j}{j_{1,a}}\right)\exp\left(\frac{F\eta}{2RT}\right) \tag{21}$$

Here, j_0 is the exchange current density and η is the overpotential can be expressed as,

For negative electrode

$$j_0 = Fk_{neg}\sqrt{c_2 c_3} \tag{22}$$

For positive electrode

$$j_0 = Fk_{pos}\sqrt{c_4 c_5} \tag{23}$$

Reaction rate constant at the positive electrode k_{pos} can be calculated by using Arrhenius law,

$$k_{pos} = k_{pos,ref}\exp\left(-\frac{FE^0_{pos}(T_{ref})}{R}\left[\frac{1}{T_{ref}} - \frac{1}{T}\right]\right) \tag{24}$$

Reaction rate constant at the negative electrode k_{neg} can be calculated by using Arrhenius law,

$$k_{neg} = k_{neg,ref}\exp\left(\frac{FE^0_{neg}(T_{ref})}{R}\left[\frac{1}{T_{ref}} - \frac{1}{T}\right]\right) \tag{25}$$

Here, $k_{neg,ref}$ and $k_{pos,ref}$ are reaction rate constants at 293 K (reference temperature). The anodic and cathodic currents, $j_{l,a}$ and $j_{l,c}$, consider the rate at which the consumed species can be brought to the electrode surface from the bulk electrolyte solution and are associated to the bulk concentration and mass transfer coefficient given by,

For negative electrode

$$j_{1,a} = -Fm_3c_3 \tag{26}$$

$$j_{1,c} = Fm_2c_2 \tag{27}$$

For positive electrode

$$j_{1,a} = -Fm_4c_4 \tag{28}$$

$$j_{1,c} = Fm_5c_5 \tag{29}$$

Where m_2, m_3, m_4, and m_5 are the mass transfer coefficients. It is assumed that mass transfer is same for each vanadium species and it is denoted by m_v. The mass transfer coefficient depends on electrolyte flow velocity v can be calculated by the following empirical equation [11]

$$m_v = 1.6 \times 10^{-4}\, v^{0.4} \tag{30}$$

Solving the nonlinear overpotential Eq. (21) requires numerical methods. If the current density is very small compared to the limiting current density so that the concentration of consumed species in the bulk solution and at the electrode surface are approximately equal, then Eq. (21) reduces to the ButlerVolmer equation [16].

$$\frac{j}{j_0} = \exp\left(-\frac{F\eta}{2RT}\right) - \exp\left(\frac{F\eta}{2RT}\right) \tag{31}$$

Above equation can be inverted to calculate the overpotential at each electrode. For negative electrode

$$\eta = \frac{2RT}{F}\sinh^{-1}\left(\frac{j}{2Fk_{neg}\sqrt{c_2c_3}}\right) \tag{32}$$

For positive electrode

$$\eta = \frac{2RT}{F}\sinh^{-1}\left(\frac{j}{2Fk_{pos}\sqrt{c_4c_5}}\right) \tag{33}$$

If the mass transfer effects are not important then Butler-Volmer equation is computationally most efficient method of approximating the overpotential. Yu and Chen [11] first time proposed new model by introducing mass transfer coefficient into the overpotential equation of the lumped model gives significant increase in overpotential, which is important in predicting the cell potential variation accurately. This model gives closed form piecewise equations to approximate current-overpotential equation over the entire range up to the limiting current.

If the current density is small with respect to limiting current density, the Butler-Volmer equation is accurate in predicting the overpotential. If the current density is high, the Butler-Volmer equation is less accurate in predicting the overpotential because it fails to capture the mass transfer effects which contributes to overpotential. Yu and Chen [11] proposed new approximations called mass transfer-limited (MTL) approximations to calculate overpotential by adding the mass transfer effects into the overpotential equation.

At high positive current densities overpotential approximations can be found by neglecting cathodic component (right side) of Eq. (21). This can be proved if the current density approaches $j_{1,a}$ at large negative overpotentials. Therefore, MTL approximations to calculate overpotential for an anodic reaction can be expressed as

$$\frac{j}{j_0} = -\left(1 - \frac{j}{j_{1,a}}\right)\exp\left(\frac{F\eta}{2RT}\right) \tag{34}$$

$$\eta = \frac{2RT}{F}\left[ln\left(\frac{j_{1,a} - j}{j}\right) + ln\left(\frac{j_{1,a}}{j_0}\right)\right] \tag{35}$$

Similarly, the MTL approximations to calculate overpotential for an cathodic reaction are

$$\frac{j}{j_0} = \left(1 - \frac{j}{j_{1,c}}\right)\exp\left(-\frac{F\eta}{2RT}\right) \tag{36}$$

$$\eta = \frac{2RT}{F}\left[ln\left(\frac{j_{1,c} - j}{j}\right) + ln\left(\frac{j_0}{j_{1,c}}\right)\right] \tag{37}$$

It is found that if the Butler-Volmer equation and MTL approximations under predicts the overpotential then larger of the two approximations should be considered for simulation [11]. In all of our simulations MTL approximations are used to calculate overpotentials.

4 Results and Discussion

All simulations are conducted by using the inhouse code. In the code, ordinary differential equations (ODE) are solved as mentioned in earlier sections. The structural dimensions of the VRFB are based on the experimental setup taken from Ref. [17]. The other parameters related to diffusion coefficients are given in Table 1 and these are reported by Tang et al. [9].

Figure 1b shows comparison between simulated and experimental cell voltage variation. The cell temperature was 297 K, initial vanadium concentration was

1200 mol/m^3, the flow rate was 1×10^{-6} m^3/s and the current density was 1000 A/m^2. The model simulated result shows very good agreement with the experimental result taken from literature for validation.

4.1 *Effects of Temperature on Diffusion Coefficients and Reaction Rate Constants*

Figure 2 shows variation of diffusion coefficients with temperature for Selemion AMV, Selemion CMV and Nafion 115 membranes. The variation of diffusion coefficients with temperature is based on the model of Arrhenius. Here the assumption is that the activation energy is same for all vanadium species. It is observed that diffusion coefficients increase with temperature, therefore change in concentration of vanadium ions takes place in both half of the cell.

The reaction rate constants also depend on temperature for both negative and positive electrode. Variation of reaction rate constant with temperature for negative and positive electrode is shown in Fig. 3a and b, respectively. The temperature dependent variation is based on Arrhenius model. It is understood from Fig. 3a that

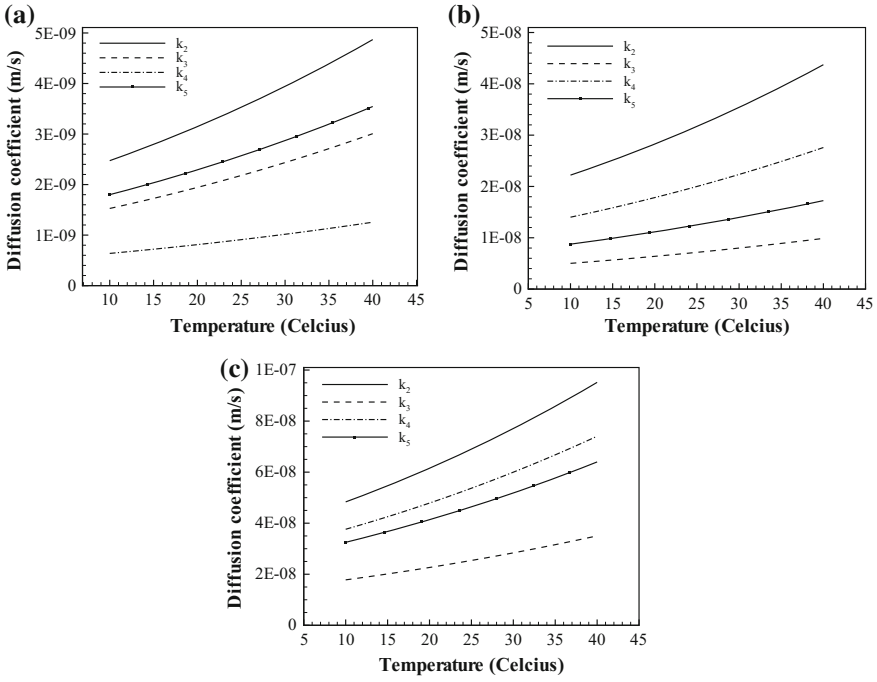

Fig. 2 Variation of membrane diffusion coefficients at different temperatures **a** Selemion AMV **b** Selemion CMV **c** Nafion 115

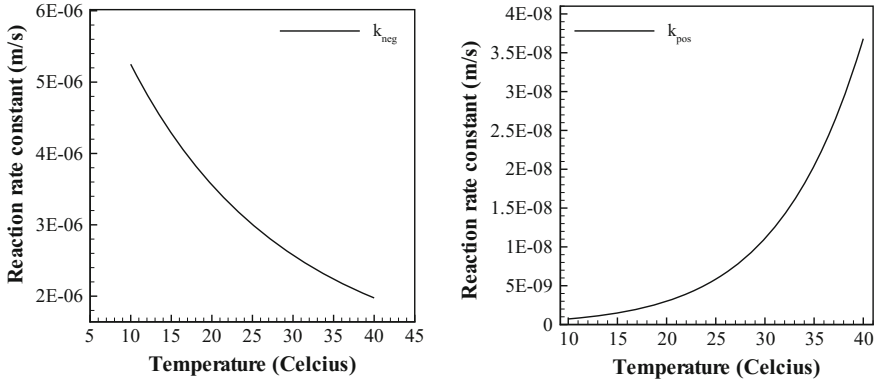

Fig. 3 Reaction rate constant at different temperatures **a** Negative electrode **b** Positive electrode

for negative electrode if temperature increases, reaction rate constant decreases, for positive electrode (see Fig. 3b) if temperature increases, reaction rate constant increases. The reaction rate constants are useful in predicting the overpotentials accurately.

4.2 Cell Potential Response for Butler-Volmer and MTL Approximations

Figure 4a shows cell potential variation with time and comparison for Butler-Volmer and MTL approximations. Higher cell voltage variation for MTL approximations is observed in comparison with Butler-Volmer equation approximations. Also it is understood that there is small difference in cell voltage between two approximations, because of adding the mass transfer term in the overpotential equation. Considering the effect of mass transfer in the model, it leads to prediction of overpotential accurately. Yu and Chen [11] showed that Butler-Volmer approximation predicts overpotential accurately for small current densities in comparison with the limiting current density. In present simulations value of current densities is high in comparison with limiting current density, therefore, MTL approximations are used.

4.3 Cell Voltage Response Due to Mass Transfer Effects

Figure 4b shows the comparison of cell potential with and without mass transfer effects state of charge (SOC) of 80% and 40 minutes discharge. If the mass transfer

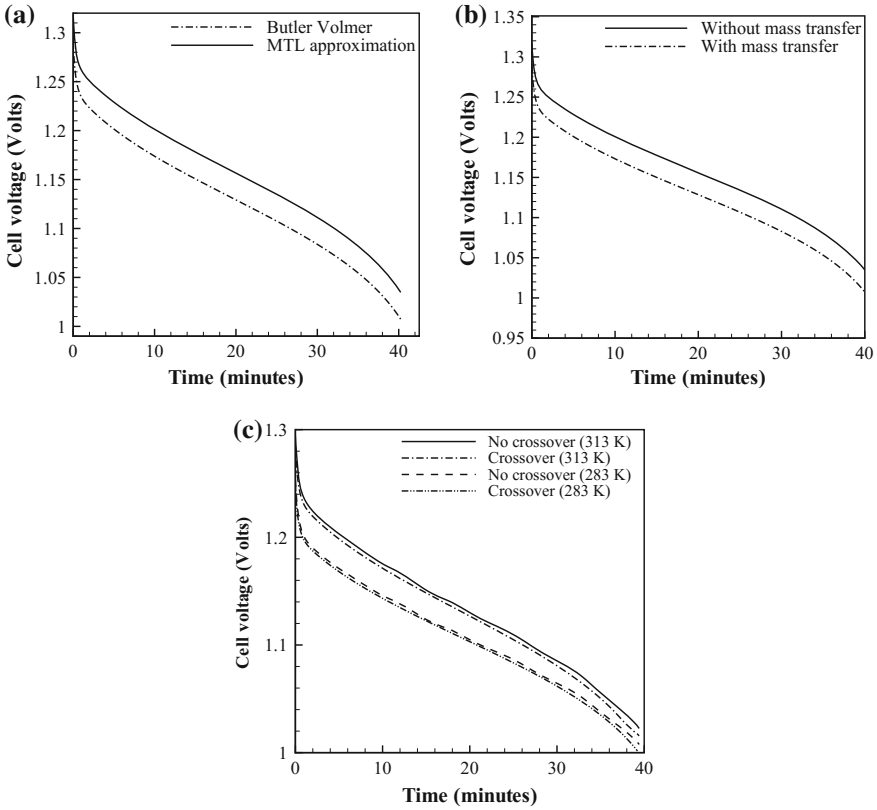

Fig. 4 **a** A comparison of Butler-Volmer equation and MTL approximation to the cell voltage. The flow rate was 1×10^{-6} m^3/s and the SOC were set to 80%. **b** Simulated discharge cell potential response with and without mass transfer effects, current density and SOC are 1000 A/m^2 and 80% respectively. **c** Simulated discharge voltage response with and without crossover at 283 K and 313 K. The flow rate and current density were set to 1 mL/s and 1000 A/m^2. The initial soc were set to 80%

effects are added and MTL approximations or Butler-Volmer equations are employed to calculate overpotential, the cell potential depends on the density ratio. When the mass transfer effects are not considered, then Butler-Volmer equations are employed to determine overpotential. It is observed that there is 2.74 mV difference between the two curves because Butler-Volmer equation used for without mass transfer effect and MTL approximations used for with mass transfer effect. The deviation is almost same till the end of discharging process. Also it is understood that cell voltage decreased by 2.74 mV due to mass transfer effect.

4.4 Cell Voltage Response Due to Crossover Effects

Figure 4c shows the comparison of cell voltage variation response with and without crossover for discharging conditions. The flow rate and current density were set to 1×10^{-6} m^3/s and 1000 A/m^2, respectively. The difference in cell potential between two cases is less for higher SOC but increases considerably for lower SOC. After discharging process, the differences in cell potential are 6 and 6.86 mV at 283 and 313 K, respectively. The difference is considerably higher for higher temperature due to increase in diffusion coefficients with temperature and it results in increase of self discharge rate. Using the cell for long term, capacity of cell decreases due to crossover and this can be overcome by electrolyte rebalancing [18]. It is observed that voltage efficiency increases with temperature because of lower activation overpotential.

4.5 Concentration Response Due to Temperature

Three different membranes such as, Selemion AMV, Selemion CMV and Nafion 115, are considered for temperature dependence solution. The upper voltage limit is assumed to be 1.7 V and lower voltage limit is 0.95 V. The vanadium species concentration for V^{2+}, V^{3+}, V^{4+} and V^{+5} are analyzed at 1.7V and temperatures ranging from 10 to 40 °C. The vanadium ion concentration variation with number of cycle trends is consistent with those diffusion model of Badrinarayanan et al. [6]. Four different vanadium ion concentrations are plotted by calculating the difference in diffusion between 10 to 40 °C as shown in Fig. 5a, b and c for three membranes (Selemion AMV, Selemion CMV and Nafion 115). Figure 6 describes the difference in vanadium concentration change between 40 and 10 °C.

The variation of concentration difference with number of cycles between 10 and 40 °C is shown in Fig. 5 for 200 charging/discharging cycles. From Fig. 5a for Selemion AMV membrane based cell, the difference in diffusion does not reduce with number of cycles but it increases with number of charging/discharging cycles. It is understood that relative difference varies linearly with number of cycles and the difference increases with the number of charging/discharging cycles. The temperature dependence characteristics curves of Selemion AMV look similar to that of Selemion CMV (Fig. 5b), but the diffusion of vanadium ion species is different.

Figure 5c shows the concentration difference with number of cycles between 40 and 10 °C for Nafion 115 membrane. It is observed that difference in diffusion increases up to 77 cycles then decreases as the number of charging/discharging cycles progresses. The diffusion of Selemion AMV and Selemion CMV does not vary linearly as it depends on the diffusion coefficient of the membrane.

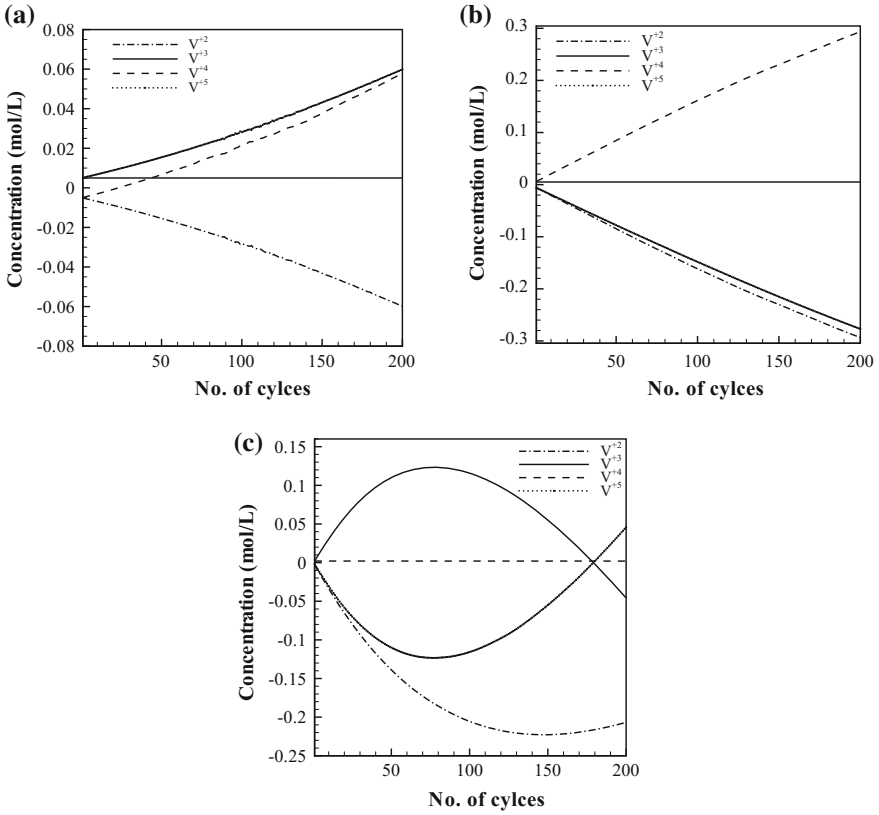

Fig. 5 Variation in diffusion trend due to temperature at 1.7 V **a** for AMV membrane **b** for CMV membrane **c** for Nafion 115 membrane

4.6 Concentration Response Due to Porosity

The variation in concentration depends on the porosity of the electrode as seen from Eqs. 10 to 13. If the porosity of the electrode varies, there is variation in the concentration which leads to changes in difference in diffusion of vanadium ions. Here three different membranes such as, Selemion AMV, Selemion CMV and Nafion 115, are also considered for porosity dependence solution. The upper cell potential limit is assumed to be 1.7 V and lower cell potential limit is 0.95 V. The vanadium species concentration for V^{2+}, V^{3+}, V^{4+} and V^{+5} are analyzed at 1.7 V at porosity values ranging from 0.6 to 0.8.

Figure 6a shows difference in diffusion variation for Selemion AMV membrane based cell, the diffusion difference increases with number of charging/discharging cycles. It is observed that for both Selemion AMV membrane and Selemion CMV

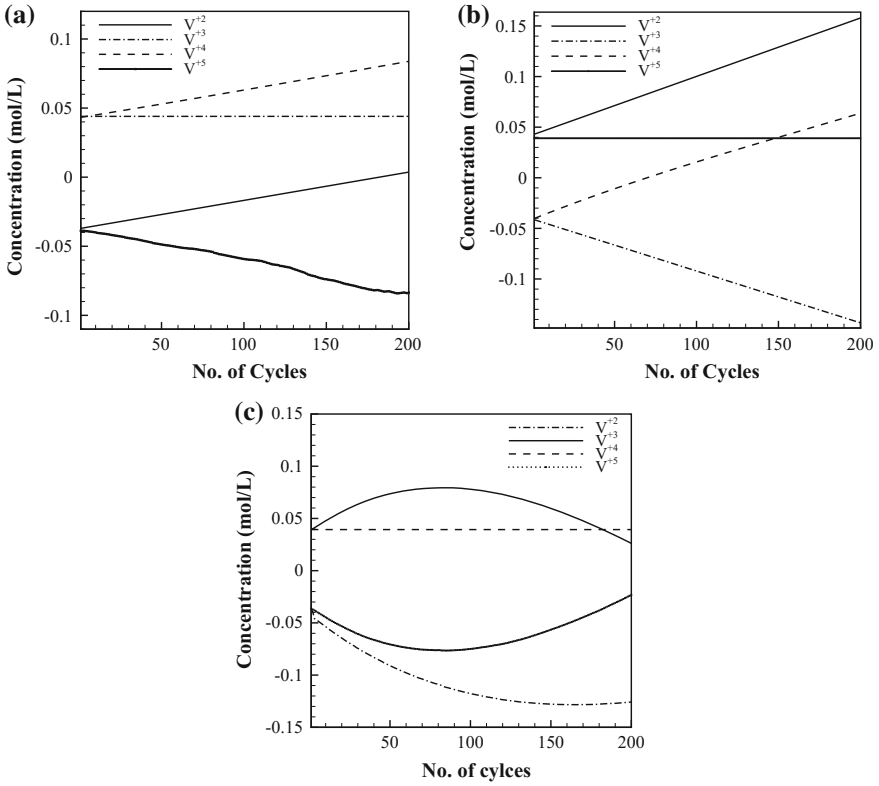

Fig. 6 Difference in diffusion trend due to porosity at 1.7 V **a** for Selemion AMV membrane **b** for Selemion CMV membrane **c** for Nafion 115 membrane

membrane (from Fig. 6b) relative difference of diffusion of concentration varies linearly with the number of cycles. The porosity dependence characteristics curves of Selemion AMV looks similar to that of Selemion CMV (Fig. 6b).

Figure 6c shows the concentration difference with number of cycles between 0.6 and 0.8 for Nafion 115 membrane. It is understood that difference in diffusion increases up to 77 cycles then decreases as the number of charging/discharging cycles increases. Also, it is observed that for current diffusion coefficient values of Nafion 115 membrane the diffusion trend is not linear compared to the other membranes (Selemion AMV membrane and Selemion CMV membrane). The cell voltage variation for 11 cycles (starting from 50 to 61) is shown in Fig. 7 for Nafion 115 membrane. It is understood that capacity of the cell decreases with charging/discharging cycles due to the effect of vanadium ions cross over through the membrane. Figure 8 shows the capacity loss of the cell variation with number of cycles for Nafion 115 membrane. It is observed that the capacity of the cell linearly

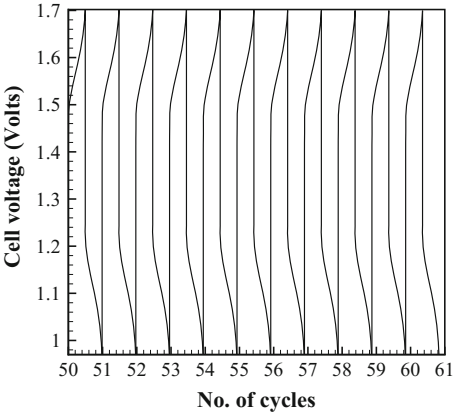

Fig. 7 Cell voltage plot for different cycles for Nafion 115 membrane for 11 cycles

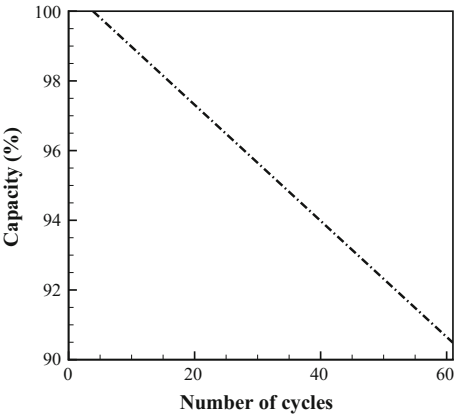

Fig. 8 Capacity versus number of cycles for Nafion 115 membrane for 60 cycles. The flow rate and current density were set to 1 mL/s and 1000 A/m^2 respectively

decreases to 90.5% after 60 cycles. Also it is noted that initial four cycles the crossover effect is very small (negligible), then decreases with number of cycles. The capacity decay is mainly due to the effect of crossover of vanadium ions through the membrane.

5 Conclusions

The present model considers the effect of mass transfer and crossover of vanadium ions through the membrane. The model is used to predict the capacity loss of the battery due to the crossover of vanadium ions through the membrane over many cycles at different temperatures. The effect of temperature and porosity on

concentration change is studied for three membrane materials such as, Selemion AMV membrane, Selemion CMV membrane and Nafion 115 membrane, the temperature ranging from 10 °C and 40 °C. Also effects of temperature on diffusion coefficients and reaction rate constants has been studied. It is observed that for Selemion AMV membrane and Selemion CMV membrane capacity loss shows linear variation with number of cycles but there is no sign of stabilizing. In the case of Nafion 115 membrane capacity loss experienced initial 77 cycles then stabilized with increase in number of cycles. The simulation results have shown that crossover and mass transfer effects have significant impact on the performance of the cell potential response. The new MTL approximations are used and predicted well the cell voltage response for higher density ratio.

Acknowledgements This study was funded by a grant from the Science and Engineering Research Board, Department of Science and Technology, the Government of India.

References

1. Skyllas-Kazacos M, Rychick M, Robins R (1988) All vanadium redox battery. US Patent No. 4 786 567, 1–22
2. Kear G, Shah AA, Walsh FC (2012) Development of the all-vanadium redox flow battery for energy storage: a review of technological, financial and policy aspects. Int J Energy Res 36:1105–1120
3. Weber AZ, Mench MM, Meyers JP, Ross PN, Gostick JT, Liu Q (2011) Redox Flow batteries: a review. J Appl Electrochem 41:1137–1164
4. Shah AA, Watt-Smith MJ, Walsh FC (2008) A dynamic performance model for redox-flow batteries involving soluble species. Electrochim Acta 53:8087–8100
5. Zhao P, Zhang H, Zhou H, Chen J, Gao S, Yi B (2006) Characteristics and performance of 10 kw class all-vanadium redox-flow battery stack. J Power Sources 162:1416–1420
6. Badrinarayanan R, Zhao J, Tseng KJ, Skyllas-Kazacos M (2014) Extended dynamic model for ion diffusion in all-vanadium redox flow battery including the effects of temperature and bulk electrolyte transfer. J Power Sources 270:576–586
7. You D, Zhang H, Sun C, Ma X (2011) Simulation of the self-discharge process in vanadium redox flow battery. J Power Sources 196:1578–1585
8. Knehr KW, Agar E, Dennison CR, Kalidindi AR, Kumbur EC (2012) A transient vanadium flow battery model incorporating vanadium crossover and water transport through the membrane. J Electrochem Soc 159(9):A1446–A1459
9. Tang A, Bao J, Skyllas-Kazacos M (2011) Dynamic modelling of the effects of ion diffusion and side reactions on the capacity loss for vanadium redox flow battery. J Power Sources 196:10737–10747
10. Tang A, Bao J, Skyllas-Kazacos M (2012) Thermal modelling of battery configuration and self-discharge reactions in vanadium redox flow battery. J Power Sources 216:489–501
11. Yu V, Chen D (2014) Dynamic model of a vanadium redox flow battery for system performance control. J Sol Energy Eng 136:0210051–0210057
12. Shah AA, Al-Fetlawi H, Walsh FC (2010) Dynamic modelling of hydrogen evolution effects in the all-vanadium redox flow battery. Electrochim Acta 55:1125–1139
13. Al-Fetlawi H, Shah AA, Walsh FC (2010) Modelling the effects of oxygen evolution in the all-vanadium redox flow battery. Electrochim Acta 55:3192–3205

14. Sun C, Chen J, Zhang H, Han X, Luo Q (2010) Investigations on transfer of water and vanadium ions across nafion membrane in an operating vanadium redox flow battery. J Power Sources 195(3):890–897
15. Springer T, Zawodzinski T, Gottesfeld S (1991) Polymer electrolyte fuel cell model. J Electrochem Soc 138(8):2334–2342
16. Newman J, Thomas-Alyea KE (2004) Electrochemical systems, A John Wiley and Sons, Inc Publication
17. Shah AA, Tangirala R, Singh R, Wills RGA, Walsh FC (2011) A dynamic unit cell model for the all-vanadium flow battery. J Electrochem Soc 158(6):A671–A677
18. Skyllas-Kazacos M, Kazacos M (2011) State of charge monitoring methods for vanadium redox flow battery control. J Power Sources 196:8822–8827